Bio-Inspired Deconjugative Isomerization of Borylated Dienoates

Amélia Messara, Byeongseok Kweon, Ferdinand Woge, Constantin G. Daniliuc, and Ryan Gilmour*

Institute for Organic Chemistry, University of Münster, Corrensstraβe 36, 48149 Münster, Germany.

Abstract: The evolutionary success of (poly)ene isomerization paradigms in generating molecular diversity is manifest throughout biosynthesis. Algorithms to relocate short π-systems, often against a thermochemical bias, with simultaneous regio- and stereo-control are a feat of precision that remain challenging to translate to a laboratory setting. The divergent biosynthesis of vitamin D and tachysterol from pre-vitamin D, leveraging positional or geometric isomerization, is a powerful exemplar. Inspired by this venerable blueprint, a deconjugative isomerization of borylated dienoates has been developed under the auspices of photochemical activation. Alleviating ground-state thermochemical restrictions through light-induced reactivity enables facile bifurcation of the diene and carbonyl chromophores: this occurs by a sequential geometric isomerization / [1,5]-hydrogen shift sequence that emulates pre-vitamin D photobiology. Broad functional group tolerance is observed, allowing the process to be leveraged in complex settings that would otherwise require multi-step approaches. It is envisaged that the operationally simple, enabling nature of this strategy, coupled with the traceless nature of the boron handle, will stimulate interest in poly(ene) relocation strategies and begin to reconcile the paucity of synthetic methods with their ubiquity in biosynthesis.

Introduction: Poly(ene) relocation algorithms are foundational biosynthetic drivers of molecular complexity, enabling short π-systems to be manipulated with iterative regio- and stereo-isomeric precision.[1] This triumph of evolution in small molecule biosynthesis mitigates the potential '*arithmetic demon*'[2] arising from multiple product formation as the π-system extends, thereby allowing subtle shunting of alkene units to occur in a thermochemically independent manner (Scheme 1A). The latitude that this platform affords is manifest throughout two-dimensional (bio)chemical space,[3] and it is often leveraged as a prelude to expedite diversity generation in three-dimensional space through substrate pre-organization. This is a central tenent of Arigoni and

Eschenmoser´s stereochemical interpretation of the isoprene rule,[4] which enables the structural repertoire of higher terpenes to be rationalized at the structural level. Despite the expansiveness of (poly)ene relocation in biology, emulating geometric[5] and positional isomerization,[6] often in a *contra*-thermodynamic direction, remains a challenging frontier in a laboratory context.[1b,7,8] This is a consequence of the energetic proximities of competing ground state process and the persistent threat posed by microscopic reversibility.[9] However, the synthetic value of these redox-neutral processes, coupled with the renaissance of light-triggered transformations that drive reactions out of equilibrium,[10] constitute powerful incentives for further investigation.

Inspired by the divergent reactivity of pre-vitamin D to generate vitamin D (via a thermal [1,7]-hydrogen shift) and tachysterol (via *Z* to *E* isomerization) (Scheme 1B),[11] it was envisaged that the key events underpinning the photobiology might be translated to a laboratory setting to induce a deconjugative isomerization of dienoates. If successful, this would enable the bifurcation of the diene and carbonyl chromophores, with a concomitant switch in hybridization from $C_\alpha(sp^2)$ to $C_\alpha(sp^3)$.

To explore the feasibility of this deconjugative process, truncated pre-vitamin D scaffolds were conceived with an integrated β-boryl acrylate motif to regulate geometric photoisomerization (**Scheme 1C**). This laboratory has recently harnessed light activation for the regio- and stereoselective geometric isomerization of borylated 1,3-dienes[12] and the positional isomerization of cyclic enones.[13] *Contra*-thermodynamic isomerization of the boryl acrylate subunit, resulting in a 90° rotation about the $C(sp^2)$-B bond to enable a stabilizing $n_O \rightarrow p_B$ interaction,[11,14] would not only ensure directionality for the transformation, but provide a traceless handle for subsequent stereospecific cross coupling.[15] It was reasoned that the configurational inversion of the first alkene unit in the β-ionyl framework,[16] would alleviate 1,3-allylic strain[17] and thereby facilitate a [1,5]-hydrogen migration. Collectively, these processes would partition the dienoate chromophore and generate a borylated diene in a manner that is reminiscent of the final stage of vitamin D biosynthesis.

Scheme 1. Motivation and conceptual framework.

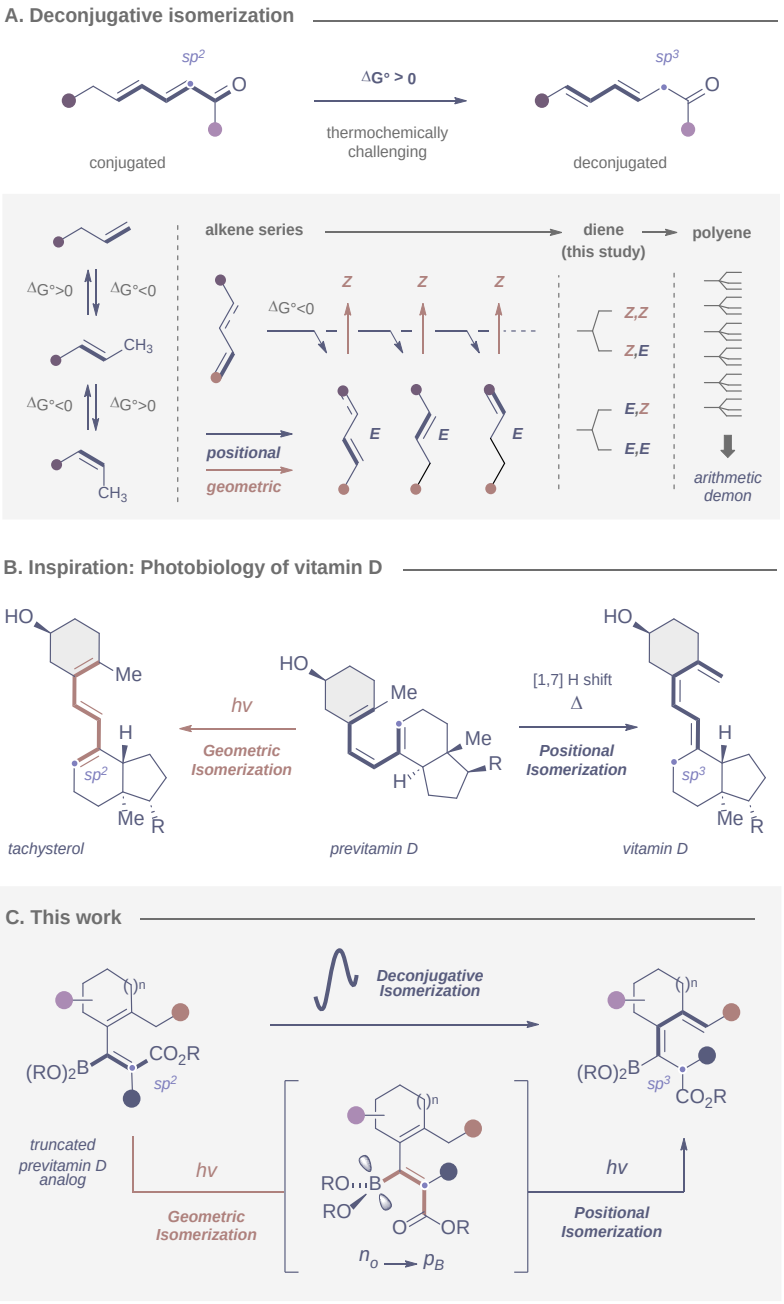

Confidence in this approach stemmed from a seminal study by Büchi and Yang, in which irradiation of β-ionone was shown to induce partial isomerization through a [1,5]-hydrogen shift.[18] More recently, Frederich and co-workers have beautifully leveraged this process to achieve photoinduced polyene cyclization cascades to convert β-ionyl derivatives into [4.4.1]-propellanes.[19] However, a major limitation of this strategy is that the scope is limited to styrenyl-based β-ionone derivatives that contain a *gem*-dimethyl functionality: deletion supresses

reactivity. Consequently, the introduction of the boron group to simultaneously modulate the chromophore, and act as a traceless steering group for conformational control, offers the opportunity to significantly broaden the scope of deconjugative dienoate isomerization under operationally simple conditions.

To explore the working hypothesis described in Scheme 1C, substrate ***Z*-1** was prepared via facile alkyne hydroboration of the corresponding enyne (please see the Supporting Information). The deconjugative isomerization of ***Z*-1** to ***Z*-2** by direct excitation was then explored at various wavelengths for 24 h in acetonitrile under an argon atmosphere (Table 1). Initial experiments under irradiation at 402 and 369 nm furnished the desired product ***Z*-2** in 22% and 50% yields, respectively (entries 1-2). The *cis*-isomer ***E*-1** was also detected in the crude mixture suggesting that geometric isomerization precedes the [1,5]-hydrogen shift (Figure 1, top). Gratifyingly, irradiation at 300 nm (performed in a Rayonet photoreactor) resulted in the highest yield of product ***Z*-2** (74%, entry 3). Reducing the reaction time to 1 h led to the formation of only traces of the desired isomer (entry 4). Although several photosensitizers were evaluated, direct excitation proved to be more effective (please see the Supporting Information).

Having identified the optimal wavelength for the title reaction, the impact of the reaction medium was explored (entries 5-8). Although toluene, EtOAc and Me-THF did not lead to an improvement (entries 5-7), 1,4-dioxane proved to be ideally suited (86%, entry 8). Control experiments were conducted to confirm the importance of light irradiation as well as the need for dry, inert conditions (entries 9-11). It is interesting to note that the generation of ***Z*-2** is accompanied by a minor isomerization of the C1-C2 alkene, but under optimal conditions this could be suppressed (entry 8). The configuration of ***Z*-2** was unequivocally established by nOe analysis and single-crystal X-ray diffraction (Figure 1, bottom; see the Supporting Information for more details). With optimal conditions having been established, the scope and limitations of the transformation were investigated (Scheme 2).

Initially, the impact of modifying the cyclohexene ring adjacent to the alkenyl boron motif was explored. The introduction of methyl or a *gem*-dimethyl groups on the ring proved unproblematic, and the target dienes ***Z*-3** and ***Z*-4** were generated with high yields and selectivities. However, the formation of the *gem*-dimethyl derivative ***Z*-4** required longer reaction times, presumably due to significant allylic strain.

Table 1. Optimization of the deconjugative isomerization.

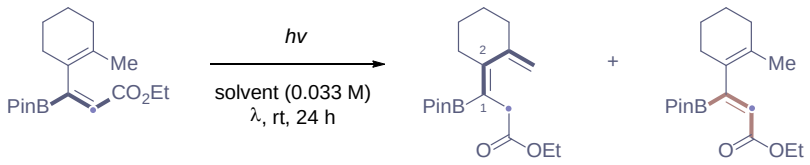

***Z*-1** ***Z*-2** ***E*-1**

Entry	λ (nm)	Solvent	Yield of *Z*-2[a] (1*Z*/1*E*)	Yield of *E*-1[a]
1	402	MeCN	22% (>95/5)	10%
2[c]	369	MeCN	50% (>95/5)	20%
3	300[b]	MeCN	74% (>95/5)	0%
4	300[b,c]	MeCN	Traces	5%
5	300[b]	Toluene	79% (92/8)	0%
6	300[b]	EtOAc	58% (>95/5)	0%
7	300[b]	Me-THF	57 (92/8)	0%
8	300[b]	1,4-Dioxane	86% (78%)[d] (>95/5)	0%
9	No light	1,4-Dioxane	0%	0%
10	300[b]	1,4-Dioxane (undried)	7%	/
11	300[b]	1,4-Dioxane (O_2 atm)	8%	/

[a] Yields and *E*:*Z* ratios were determined by ^{1}H NMR spectroscopy using 1,3,5-trimethoxybenzene as an internal standard. The *Z*:*E* assignment of the alkene follows IUPAC nomenclature and reflects the priority C > B. [b] Reaction performed in a Rayonet photoreactor at 35 °C. [c] Reaction performed for 1 h. [d] Isolated yields given in parentheses.

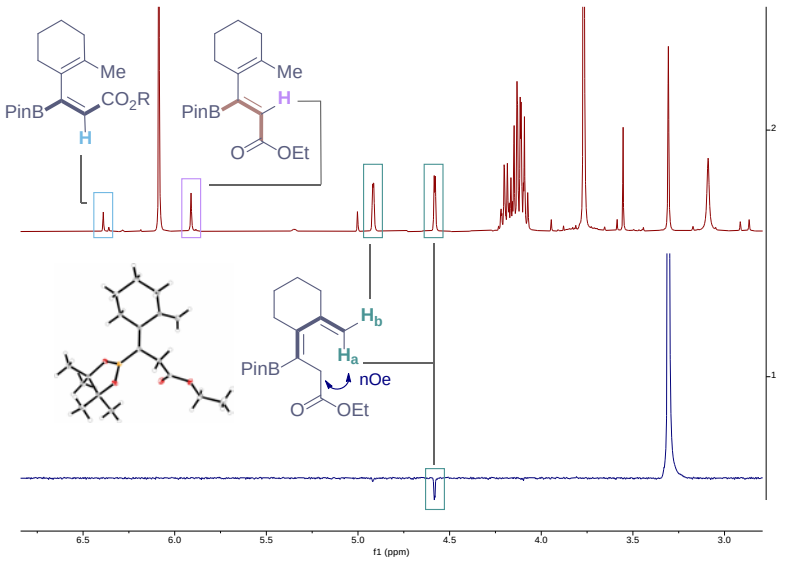

Figure 1. Crude ^{1}H NMR spectrum (400 MHz, $CDCl_3$) of the photo-reaction after 24 h at 402 nm (in red); Insert: Crystal structure of compound ***Z*-2** (CCDC 2467356)[21] and nOe analysis (in blue).

Oxygen- and nitrogen-containing heterocycles (e.g., ***Z*-5** and ***Z*-6**) were well tolerated under the reaction conditions, and medium rings proved to be highly compatible. Gratifyingly, ***Z*-7** and ***Z*-8** could be generated efficiently (up to 1*Z*/1*E* >95:5) in just 8 h instead of 24 h. Despite the extended chromophore in the dihydronaphthalene substrate, ***E*-9** could be formed albeit with a lower selectivity (1*E*/1*Z* = 62:38). Pleasingly these operationally simple conditions allowed more complex scaffolds to be modified such as the camphor derivative ***Z*-10** and the cholestenone derivative ***Z*-11**. Collectively, these examples (***Z*-2** to ***Z*-11**) demonstrate that the method does not require the proximal *gem*-dimethyl group in the substrate. To further establish generality of substrate scope, the methyl group of ***Z*-1** was systematically replaced by other substituents. Gratifyingly, the introduction of isopropyl and cyclohexyl substituents did not impact selectivity of the reaction (1*Z*/1*E* >95:5 for ***Z*-12** and ***Z*-13**). The introduction of simple alkyl chains was also well-tolerated (***Z*-14**-**16**), but this led to the generation of C3–C4 isomers which were easily separable by column chromatography. Notably, the introduction of a bulky phthalimide substituent (***Z*-17**) ensured high levels of geometric control at both C1-C2 and C3–C4 following deconjugative isomerization.

Variation of the ester moiety was generally very well tolerated (e.g., ***Z*-18**-**22**) and the introduction of more complex scaffolds such as cholesterol, menthol and geraniol had no impact on the yield or selectivity of the transformation (***Z*-23**-**25**, up to 97% and 1*Z*/1*E* >95:5). The incorporation of a methyl group at the □-position of the ester unit was unproblematic, furnishing the desired product ***Z*-26** in high yield (1*Z*/1*E* >95:5). An interesting observation resulted from the replacement of the BPin motif with a BMIDA, enabling compound ***Z*-27** to be generated in 80% yield with an excellent selectivity. In contrast to the BPin motif containing a vacant *p*-orbital that can engage with the carbonyl oxygen to bias the geometric isomerization, the *p*-orbital in the BMIDA is occupied (*vide infra*).

To interrogate the constituent events that enable this deconjugative isomerization of dienoates, a series of mechanistic investigations were performed (Figure 2). Initially, the *cis*-isomer ***E*-1** was independently prepared (see Supporting Information),[20] and the UV absorption spectra of the individual isomers (***Z*-1**, ***E*-1**, and ***Z*-2**) were recorded (Figure 2A).

Scheme 2. Evaluation of substrate scope in the deconjugative isomerization of borylated dienoates.[a]

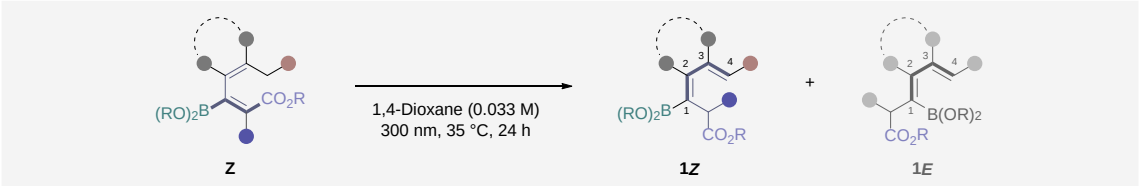

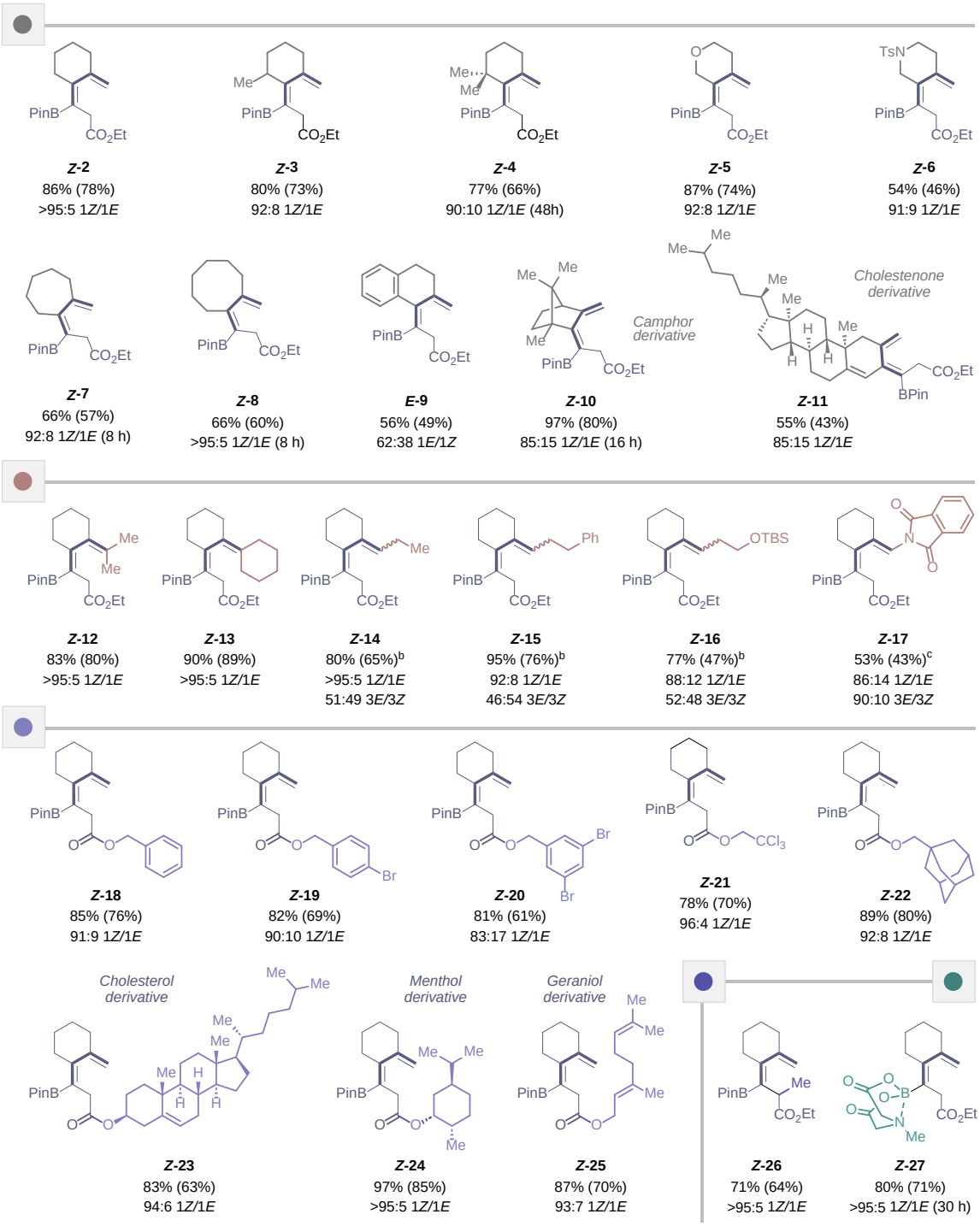

Z-2
86% (78%)
>95:5 1Z/1E

Z-3
80% (73%)
92:8 1Z/1E

Z-4
77% (66%)
90:10 1Z/1E (48h)

Z-5
87% (74%)
92:8 1Z/1E

Z-6
54% (46%)
91:9 1Z/1E

Z-7
66% (57%)
92:8 1Z/1E (8 h)

Z-8
66% (60%)
>95:5 1Z/1E (8 h)

E-9
56% (49%)
62:38 1E/1Z

Z-10
97% (80%)
85:15 1Z/1E (16 h)

Z-11
55% (43%)
85:15 1Z/1E

Z-12
83% (80%)
>95:5 1Z/1E

Z-13
90% (89%)
>95:5 1Z/1E

Z-14
80% (65%)[b]
>95:5 1Z/1E
51:49 3E/3Z

Z-15
95% (76%)[b]
92:8 1Z/1E
46:54 3E/3Z

Z-16
77% (47%)[b]
88:12 1Z/1E
52:48 3E/3Z

Z-17
53% (43%)[c]
86:14 1Z/1E
90:10 3E/3Z

Z-18
85% (76%)
91:9 1Z/1E

Z-19
82% (69%)
90:10 1Z/1E

Z-20
81% (61%)
83:17 1Z/1E

Z-21
78% (70%)
96:4 1Z/1E

Z-22
89% (80%)
92:8 1Z/1E

Z-23
83% (63%)
94:6 1Z/1E

Z-24
97% (85%)
>95:5 1Z/1E

Z-25
87% (70%)
93:7 1Z/1E

Z-26
71% (64%)
>95:5 1Z/1E

Z-27
80% (71%)
>95:5 1Z/1E (30 h)

[a] Reaction conditions: Substrate (0.1 or 0.2 mmol), 1,4-dioxane (0.033 M), 300 nm irradiation using a Rayonet photoreactor at 35 °C, 24 h, Ar atmosphere. Yields and *E:Z* ratios were determined by 1H NMR using 1,3,5-trimethoxybenzene as an internal standard. Isolated yields given in parenthesis for the major isomer **1*Z***; [b] Combined isolated yields given for the two isomers (1*Z*,3*E* and 1*Z*,3*Z*), see Supporting Information for additional details; [c] Isolated yield given for the isomer 1*Z*,

Both ***Z*-1** and ***E*-1** exhibit absorption bands around 300 nm, with ***E*-1** displaying a notably enhanced intensity. In contrast, the [1,5]-adduct ***Z*-2** displayed no significant absorption in this region, thereby preventing re-excitation and leading to accumulation. To glean additional structural information, the benzyl ester series (***Z*-28**, ***E*-28**, ***Z*-18**) were crystallized and their structures were unequivocally established by X-ray diffraction analysis (Figure 2B).[21] In the starting material (***Z*-28**), the boron atom is conjugated to the adjacent α,β-unsaturated ester, resulting in a planar conjugated system. Following geometric photoisomerization, the product ***E*-28** displays a stabilizing $n_O \rightarrow p_B$ interaction arising from a 90° rotation of the C(sp^2)–B bond.[14a] This interaction likely accounts for the increased absorption of the *E*-isomer. Finally, X-ray analysis of the [1,5]-product (***Z*-2**, Figure 1 and ***Z*-18**, Figure 2B) illustrates the bifurcation of the diene and the ester chromophores, with a net change in hybridization of C1 from C(sp^2) to C(sp^3).

To explore the impact of isomerization on the net process, and provide support for the relevance of geometric isomerization in expediting the [1,5]-shift, the formation of ***Z*-2** from either the *trans*-isomer ***Z*-1** or the *cis*-isomer ***E*-1** was monitored by ^{1}H NMR spectroscopy (Figure 2C). Comparable yields of ***Z*-2** were obtained from both ***Z*-1** and ***E*-1**, but starting from the isomerized species significantly reduced the reaction time to 6 h. These results indicate that geometric isomerization is beneficial for deconjugative isomerization. The shorter reaction times associated with ***E*-1** can be attributed to the enhanced absorption resulting from favorable structural preorganization: this also facilitates the [1,5]-hydrogen shift.

Establishing whether or not the [1,5]-hydrogen shift proceeded thermally[22] was achieved by exposing the conjugated dienoates to elevated temperatures (Figure 2D). Independently heating ***Z*-1** or ***E*-1** to 90 °C or 150 °C did not yield the product ***Z*-2**: this effectively excludes a thermally induced transformation. This suggests that the reaction proceeds photochemically, opening up the possibilities of radical and pericyclic mechanisms.[23] Interestingly, when ***Z*-2** was subjected to elevated temperatures (150 °C), generation of ***Z*-1** (25%) and ***E*-1** (67%) was observed, likely through a retro-[1,5]-hydrogen shift (Figure 2D).

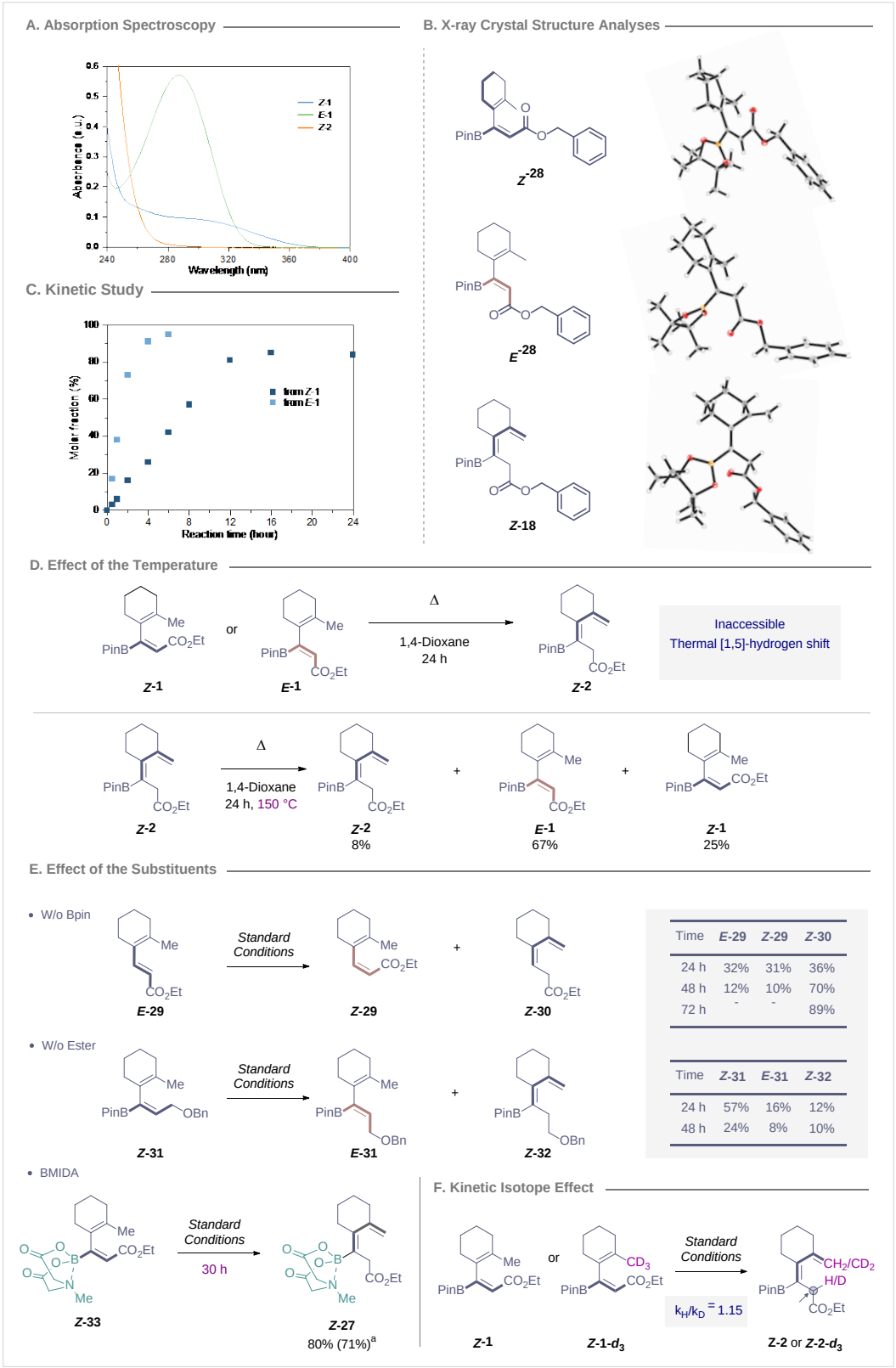

Figure 2. Mechanistic experiments. A. Absorption spectra of ***Z*-1**, ***E*-1** and ***Z*-2** (in MeCN); B. X-ray crystal analyses of ***Z*-28**, ***E*-28** and ***Z*-18**; C. Kinetic study of the photoreaction starting from either the *trans*-isomer ***Z*-1** or the *cis*-isomer ***E*-1**; D. Impact of the temperature; E. Effect of the substituents; F. Kinetic isotope effect. Yields were determined by ^{1}H NMR using 1,3,5-trimethoxybenzene as an internal standard. [a] Isolated yield given in parentheses after 30 h instead of 24 h.

These findings underscore the value of photochemical activation in this context, where disruption of the chromophore in ***Z*-2** prevents further excitation and thus mitigates reverse reactions that compromise efficiency. This conclusion is supported by UV absorption spectroscopy measurements as shown in Figure 2A, and is in-line with observations reported for β-ionyl derivatives.[16d,19]

A major driving force behind this study was to address the existing scope limitations of deconjugative dienoate isomerization and therefore a series of molecular deletions were conducted (Figure 2E). Initially, the BPin handle was removed to illustrate its role in the process. When starting from compound ***E*-29**, the desired product ***Z*-30** was obtained in only 36% yield after 24 h, highlighting its importance. The carbonyl group proved to be crucial, such that irradiation of compound ***Z*-31** delivered only 10% of the target product ***Z*-32** after 48 h. These findings underscore the importance of the substituents in enabling the transformation and support the working hypothesis that the boron moiety effectively emulates the effect of the *gem*-dimethyl group inherent to naturally occurring β-ionyl systems, and that it clearly imparts additional physicochemical benefits for photoactivation such as notably enhancement in absorption (see Figure 2A). To further probe the role of the $n_O \rightarrow p_B$ interaction, the Bpin group was replaced by a BMIDA substituent, in which the boron *p*-orbital is effectively occupied in the substrate and product. Based on our previous studies on the geometric isomerization of boryl acrylates,[12,14] this derivative was anticipated to be poorly or non-reactive under the standard conditions. Nevertheless, as noted above (Figure 2), the isomerized diene product ***Z*-27** was obtained efficiently. Importantly, however, elongated reaction times were required (30 h instead of 16 h) further indicating the value of geometric isomerization in facilitating the [1,5]-hydrogen shift. Finally, a kinetic isotope effect (KIE) experiment revealed that the [1,5]-hydrogen shift is not the rate-limiting step in this photochemical cascade (Figure 2F). Whilst reaction progress monitoring has revealed obvious differences in the reaction times between the *E*- and *Z*-starting material isomers, the subtlety of these effects is favorable from an operational perspective and confers a high degree of latitude.

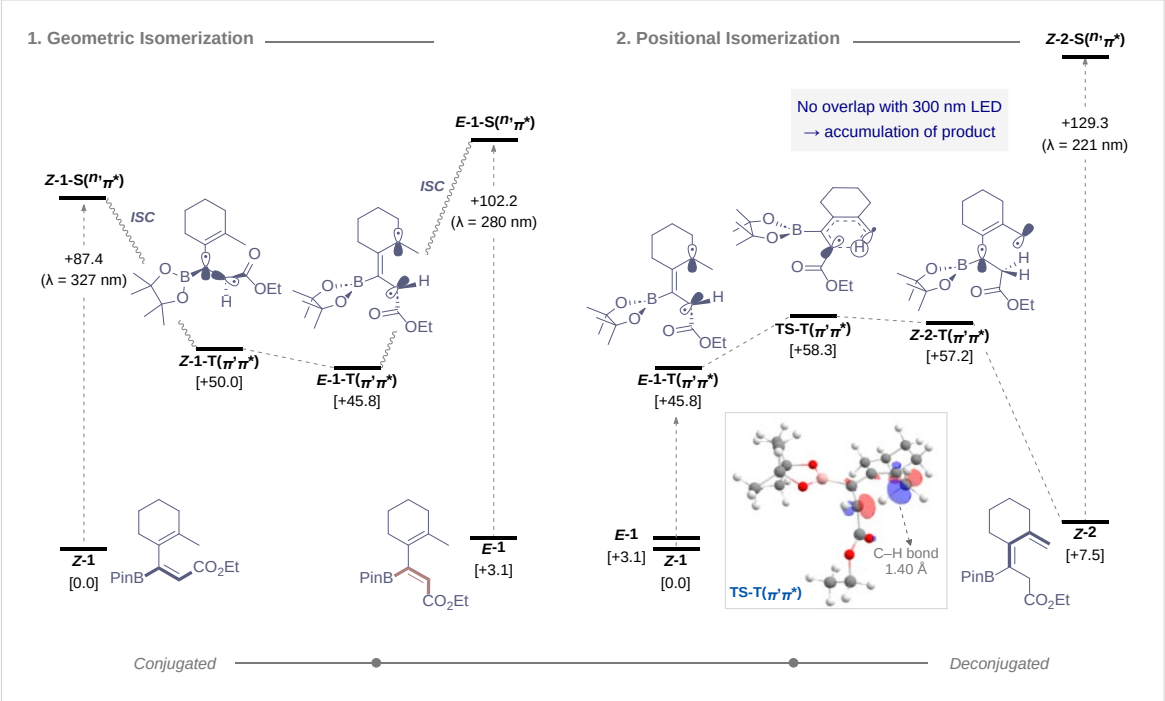

Figure 3. Computational investigations of the photochemical deconjugative isomerization. TD-DFT: CAM-B3LYP / def2-TVZP, ΔG_{203}(1,4-dioxane)/(kcal mol^{-1}): MO62X / def2-SVP / def2-TZVP.

To interrogate the possibilities of a pericyclic pathway or a radical [1,5]-hydrogen atom transfer, computational studies were conducted (Figure 3). Initially, the geometric isomerization of ***Z*-1** to ***E*-1** was considered. Under the optimized reaction conditions reported in this study, both isomers are excited to the singlet n,π* state, followed by intersystem crossing (ISC) to the triplet π,π* state. Notably, the triplet energy of ***E*-1-T(π,π*)** was calculated to be 4.2 kcal/mol lower than that of ***Z*-1-T(π,π*)**, indicating that the *contra*-thermodynamic isomerization from ***Z*-1** to ***E*-1** is feasible.

Upon continued irradiation, ***E*-1-T(π,π*)** is proposed to undergo a [1,5]-hydrogen migration process. The electrophilic radical located at the 𝛽-carbonyl position facilitates an intramolecular hydrogen atom transfer (HAT) from the methyl substituent with an activation barrier of 12.5 kcal/mol. This leads to the formation of a biradical intermediate, which is stabilized through the α-boryl radical effect,[24] providing a mechanistic rationale for the observed acceleration of positional isomerization in the presence of the boronate group. The intermediate then proceeds through the product triplet state and ultimately converges on the final product ***Z*-2**. Time-dependent DFT (TD-DFT) calculations revealed that, unlike the two geometric isomers, the deconjugated product exhibits a significantly higher

excitation energy (129.3 kcal/mol, 5.61 eV, 221 nm) due to its large HOMO–LUMO gap. This value exceeds the emission range of the LED light source used under the standard reaction conditions, as the absorption spectrum of the product does not overlap with the LED emission profile. Consequently, the product cannot be re-excited and selectively accumulates among the three possible isomers, ultimately becoming the dominant species under continuous irradiation. While these computational studies and mechanistic investigations strongly support a photochemically driven sequential isomerization process followed by intramolecular hydrogen atom transfer, the contribution of alternative mechanisms, such as a pericyclic [1,5]-sigmatropic rearrangement, cannot be completely excluded.[22b,23]

Scheme 3. Selected derivatization reactions of *Z*-2.[a]

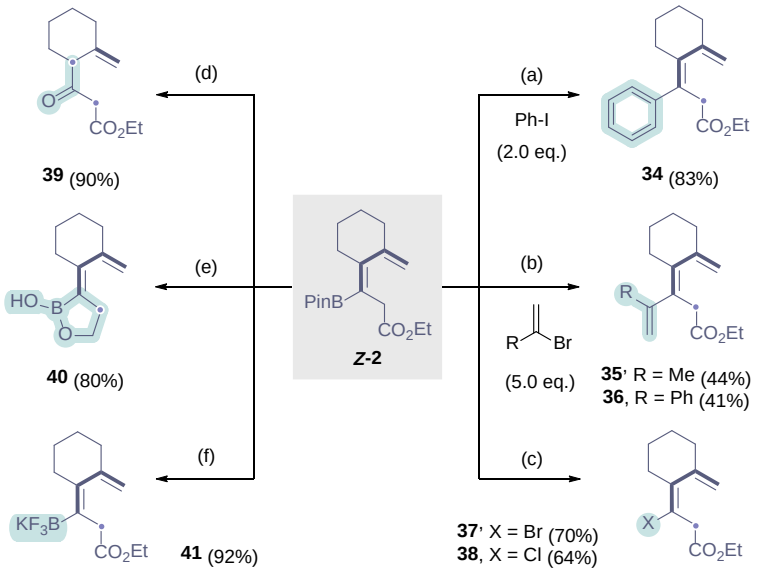

[a] Reaction conditions: (a) $Pd(dppf)Cl_2$ (2 mol%), Na_2CO_3 (3.0 eq.), 1,4-dioxane/H_2O (5:1), 90 °C, 16 h; (b) $Pd(PPh_3)_4$ (20 mol%), NaOMe (3.0 eq.), Toluene/MeOH (4:1), 80 °C, 24 h; (c) CuX_2 (2.0 eq.), THF/H_2O (1:1), 70 °C, 16 h; (d) H_2O_2/NaOH, THF, rt, 3 h; (e) $NaBH_4$ (2.5 eq.), EtOH, rt, 2.5 h, (f) KHF_2 (3.0 eq.), MeOH/H_2O (2:1), rt, 1 h.

Finally, to demonstrate the synthetic utility of the borylated diene products generated by this deconjugative process, a series of derivatization reactions were explored (Scheme 3). Suzuki-Miyaura cross-couplings were successfully performed to introduce either aryl or alkene units (**34** - **36**). Halogenation of compound ***Z*-2** proved to be facile to enable generation of the corresponding bromo-

and chloro-derivatives **37** and **38**. To our delight, oxidation of the Bpin group afforded ketone **39** in 90% yield, in which the three short chromophores are partitioned by C(sp^3) units. No observable isomerization of the exocyclic double bond was observed rendering the approach orthogonal to methods that lead to the generation of the α,β-unsaturated ketone.[25] Under reductive conditions, the pharmaceutically relevant[26] oxaborole scaffold **40** was isolated in 80% yield. Additionally, boronic ester protection enabled the formation of the corresponding trifluoroborate **41**.

Conclusions: The photobiology of pre-vitamin D has inspired the development of a deconjugative isomerization of dienoates with concomitant regulation of alkene geometry. Under the auspices of photochemical irradiation, this operationally simple protocol leverages borylated substrates in which the traceless BPin facilitates chromophore bifurcation in the target product, thereby imparting directionality and mitigating the generation of structural isomers. The process displays a high degree of generality as is exemplified by a scope which includes terpene and steroid derivatives that would otherwise require multistep syntheses to access. Mechanistic investigations and computational studies suggested a pathway involving an initial *contra*-thermodynamic geometric isomerization, followed by a radical [1,5]-hydrogen migration, and structural deletion experiments highlight the importance of the boron and ester groups. Although the development of poly(ene) relocation strategies that approach biological levels of precision remain a challenge goal, the ease with which photochemical activation enable complex scaffolds to be manipulated is a compelling driver for further investigation.

Corresponding Author

ryan.gilmour@uni-muenster.de

Author Contributions

The manuscript was written through contributions of all authors. All authors have given approval to the final version of the manuscript.

ACKNOWLEDGMENT

We acknowledge generous financial support from the University of Münster, the Alexander von Humboldt Foundation (Fellowship to AM) and the European Union H2020 research and innovation program under the Marie S. Curie Grant Agreement (PhotoReAct, No 956324, BK).

REFERENCES

1. (a) Dugave, C.; Demange, L. Cis–Trans Isomerization of Organic Molecules and Biomolecules: Implications and Applications. *Chem. Rev.* **2003**, *103*, 2475–2532; (b) Neveselý, T.; Wienhold, M.; Molloy, J. J.; Gilmour, R. Advances in the *E* → *Z* Isomerization of Alkenes Using Small Molecule Photocatalysts. *Chem. Rev.* **2022**, *122*, 2650–2694.

2. (a) Sharpless, K. B. Synthesis of Erythro-18,19-Dihydroxysqualene 2,3-Oxide and Other Internally Oxidized Squalene Derivatives. *J. Chem. Soc. D Chem. Commun.* **1970**, *21*, 1450–1451; (b) Sharpless, K. B. D,L-Malabaricanediol. The First Cyclic Natural Product Derived from Squalene in a Nonenzymic Process. *J. Am. Chem. Soc.* **1970**, *92*, 6999–7001; (c) Crispino, G. A.; Ho, P. T.; Sharpless, K. B. Selective Perhydroxylation of Squalene: Taming the Arithmetic Demon. *Science* **1993**, *259*, 64–66.

3. (a) Zechmeister, L. Cis-Trans Isomerization and Stereochemistry of Carotenoids and Diphenyl-Polyenes. *Chem. Rev.* **1944**, *34*, 267–344; (b) Wyman, G. M. The *Cis-Trans* Isomerization of Conjugated Compounds. *Chem. Rev.* **1955**, *55*, 625–657; (c) Thirsk, C.; Whiting, A. Polyene Natural Products. *J. Chem. Soc., Perkin Trans. 1* **2002**, *8*, 999–1023; (d) Moise, A. R.; Al-Babili, S.; Wurtzel, E. T. Mechanistic Aspects of Carotenoid Biosynthesis. *Chem. Rev.* **2014**, *114*, 164–193; (e) Chatgilialoglu, C.; Ferreri, C.; Melchiorre, M.; Sansone, A.; Torreggiani, A. Lipid Geometrical Isomerism: From Chemistry to Biology and Diagnostics. *Chem. Rev.* **2014**, *114*, 255–284.

4. (a) Ruzicka, L. The isoprene rule and the biogenesis of terpenic compounds. *Experientia* **1953**, *9*, 357–367; (b) Eschenmoser, A.; Ruzicka, L.; Jeger, O.; Arigoni, D. Eine stereochemische Interpretation

der biogenetischen Isoprenregel bei den Triterpenen. *Helv. Chim. Acta* **1955**, *38*, 1890–1904; (c) Eschenmoser, A.; Arigoni, D. Revisited after 50 Years: The stereochemical interpretation of the biogenetic isoprene rule for the triterpenes. *Helv. Chim. Acta* **2005**, *88*, 3011–3048; (d) Stork, G.; Burgstahler, A. W. The Stereochemistry of Polyene Cyclization. *J. Am. Chem. Soc.* **1955**, *77*, 5068–5077; (e) Stadler, P. A.; Eschenmoser, A.; Schinz, H.; Stork, G. Untersuchungen Über Den Sterischen Verlauf Säurekatalysierter Cyclisationen Bei Terpenoiden Polyenverbindungen. 3. Mitteilung. Zur Stereochemie Der Bicyclofarnesylsäuren. *Helv. Chim. Acta* **1957**, *40*, 2191–2198; (f) Cornforth, J. W. The biosynthesis of polyisoprenoids. *Pure Appl. Chem*. **1961**, *2*, 607–630.

5. For selected examples of geometric photoisomerization, see: (a) Singh, K.; Staig, S. J.; Weaver, J. D. Facile Synthesis of Z-Alkenes via Uphill Catalysis. *J. Am. Chem. Soc.* **2014**, *136*, 5275–5278; (b) Metternich, J. B.; Gilmour, R. A Bio-Inspired, Catalytic the *E* → *Z* Isomerization of Activated Olefins. *J. Am. Chem. Soc.* **2015**, *137*, 11254–11257; (c) Metternich, J. B.; Gilmour, R. One Photocatalyst, n Activation Modes Strategy for Cascade Catalysis: Emulating Coumarin Biosynthesis with (−)-Riboflavin. *J. Am. Chem. Soc.* **2016**, *138*, 1040–1045; (d) Metternich, J. B.; Artiukhin, D. G.; Holland, M. C.; von Bremen-Kühne, M.; Neugebauer, J.; Gilmour, R. Photocatalytic *E* → *Z* Isomerization of Polarized Alkenes Inspired by the Visual Cycle: Mechanistic Dichotomy and Origin of Selectivity. *J. Org. Chem.* **2017**, *82*, 9955–9977; (e) Cai, W.; Fan, H.; Ding, D.; Zhang, Y.; Wang, W. Synthesis of Z-Alkenes via Visible Light Promoted Photocatalytic *E* → *Z* Isomerization under Metal-Free Conditions. *Chem. Commun.* **2017**, *53*, 12918–12921; (f) Molloy, J. J.; Metternich, J. B.; Daniliuc, C. G.; Watson, A. J. B.; Gilmour, R. Contra-Thermodynamic, Photocatalytic *E* → *Z* Isomerization of Styrenyl Boron Species: Vectors to Facilitate Exploration of Two-Dimensional Chemical Space. *Angew. Chem. Int. Ed.* **2018**, *57*, 3168–3172; (g) Kurzawa, T.; Harms, K.; Koert, U. Stereoselective Synthesis of the Benzodihydropentalene Core of the Fijiolides. *Org. Lett.* **2018**, *20*, 1388–1391; (h) Faßbender, S. I.; Molloy, J. J.; Mück-Lichtenfeld, C.; Gilmour, R. Geometric *E* → *Z* Isomerisation of Alkenyl Silanes by Selective Energy Transfer Catalysis: Stereodivergent Synthesis of Triarylethylenes via a Formal Anti-Metallometallation. *Angew. Chem. Int. Ed.* **2019**, *58*, 18619–18626; (i) Neveselý, T.; Daniliuc, C. G.; Gilmour, R. Sequential Energy Transfer

Catalysis: A Cascade Synthesis of Angularly-Fused Dihydrocoumarins. *Org. Lett.* **2019**, *21*, 9724–9728; (j) Onneken, C.; Bussmann, K.; Gilmour, R. Inverting External Asymmetric Induction via Selective Energy Transfer Catalysis: A Strategy to β-Chiral Phosphonate Antipodes. *Angew. Chem. Int. Ed.* **2020**, *59*, 330–334; (k) Neveselý, T.; Molloy, J. J.; McLaughlin, C.; Brüss, L.; Daniliuc, C. G.; Gilmour, R. Leveraging the n→π* Interaction in Alkene Isomerization by Selective Energy Transfer Catalysis. *Angew. Chem. Int. Ed.* **2022**, *61*, e202113600.

6. For selected reviews on positional isomerization, see: (a) Vasseur, A.; Bruffaerts, J.; Marek, I. Remote Functionalization through Alkene Isomerization. *Nature Chem.* **2016**, *8*, 209–219; (b) Liu, X.; Li, B.; Liu, Q. Base-Metal-Catalyzed Olefin Isomerization Reactions. *Synthesis* **2019**, *51*, 1293–1310; (c) Massad, I.; Marek, I. Alkene Isomerization through Allylmetals as a Strategic Tool in Stereoselective Synthesis. *ACS Catal.* **2020**, *10*, 5793–5804; (d) Fiorito, D.; Scaringi, S.; Mazet, C. Transition Metal-Catalyzed Alkene Isomerization as an Enabling Technology in Tandem, Sequential and Domino Processes. *Chem. Soc. Rev.* **2021**, *50*, 1391–1406.

7. (a) Metternich, J. B.; Gilmour, R. Photocatalytic *E* → *Z* Isomerization of Alkenes. *Synlett* **2016**, *27*, 2541–2552; (b) Molloy, J. J.; Morack, T.; Gilmour, R. Positional and Geometrical Isomerisation of Alkenes: The Pinnacle of Atom Economy. *Angew. Chem. Int. Ed.* **2019**, *58*, 13654–13664; (c) Corpas, J.; Mauleón, P.; Gómez Arrayás, R.; Carretero, J. C. *E*/*Z* Photoisomerization of Olefins as an Emergent Strategy for the Control of Stereodivergence in Catalysis. *Adv. Synth. Catal.* **2022**, *364*, 1348–1370; (d) Wang, P.-Z.; Xiao, W.-J.; Chen, J.-R. Light-empowered *contra*-thermodynamic stereochemical editing. *Nat. Rev. Chem.* **2023**, *7*, 35−50.

8. For selected examples on deconjugative isomerization of alkenes, see: (a) Jorgenson, M. J. Photochemical Hydrogen Abstraction in Unsaturated Esters. *Chem. Commun.* **1965**, 137–138; (b) Duhaime, R. M.; Lombardo, D. A.; Skinner, I. A.; Weedon, A. C. Conversion of α,β-Unsaturated Esters to Their β,γ-Unsaturated Isomers by Photochemical Deconjugation. *J. Org. Chem.* **1985**, *50*, 873–879;

(c) Pete, J.-P.; Henin, F.; Mortezaei, R.; Muzart, J.; Piva, O. Enantioselective Photodeconjugation of Conjugated Esters and Lactones. *Pure Appl. Chem.* **1986**, *58*, 1257–1262; (d) Arnold, D. R.; Mines, S. A. Radical Ions in Photochemistry. 18. The Photosensitized (Electron Transfer) Tautomerization of Alkenes; the 1,1-Diphenyl Alkene System. *Can. J. Chem.* **1987**, *65*, 2312–2314; (e) Piva, O.; Mortezaei, R.; Henin, F.; Muzart, J.; Pete, J. P. Highly Enantioselective Photodeconjugation of α,β-Unsaturated Esters. Origin of the Chiral Discrimination. *J. Am. Chem. Soc.* **1990**, *112*, 9263–9272; (f) Mangion, D.; Kendall, J.; Arnold, D. R. Photosensitized (Electron-Transfer) Deconjugation of 1-Arylcyclohexenes. *Org. Lett.* **2001**, *3*, 45–48; (g) Morack, T.; Onneken, C.; Nakakohara, H.; Mück-Lichtenfeld, C.; Gilmour, R. Enantiodivergent Prenylation via Deconjugative Isomerization. *ACS Catal.* **2021**, *11*, 11929–11937; (h) Occhialini, G.; Palani, V.; Wendlandt, A. E. Catalytic, Contra-Thermodynamic Positional Alkene Isomerization. *J. Am. Chem. Soc.* **2022**, *144*, 145–152; (i) Zhao, K.; Knowles, R. R. Contra-Thermodynamic Positional Isomerization of Olefins. *J. Am. Chem. Soc.* **2022**, *144*, 137–144; (j) Palani, V.; Wendlandt, A. E. Strain-Inducing Positional Alkene Isomerization. *J. Am. Chem. Soc.* **2023**, *145*, 20053–20061.

9. Tolman, R. C. The Principle of Microscopic Reversibility. *Proc. Natl. Acad. Sci. U. S. A.* **1925**, *11*, 436–439.

10. (a) Kathan, M.; Hecht, S. Photoswitchable Molecules as Key Ingredients to Drive Systems Away from the Global Thermodynamic Minimum. *Chem. Soc. Rev.* **2017**, *46*, 5536–5550; (b) Ota, E.; Wang, H.; Frye, N. L.; Knowles, R. R. A Redox Strategy for Light-Driven, Out-of-Equilibrium Isomerizations and Application to Catalytic C–C Bond Cleavage Reactions. *J. Am. Chem. Soc.* **2019**, *141*, 1457–1462.

11. (a) Holick, M. F.; MacLaughlin, J. A.; Doppelt, S. H. Regulation of Cutaneous Previtamin D3 Photosynthesis in Man: Skin Pigment Is Not an Essential Regulator. *Science* **1981**, *211*, 590–593; (b) Yamamoto, J. K.; Borch, R. F. Photoconversion of 7-Dehydrocholesterol to Vitamin D3 in Synthetic Phospholipid Bilayers. *Biochemistry* **1985**, *24*, 3338–3344 (c) Holick, M. F. Vitamin D Deficiency. *N. Engl.*

J. Med. **2007**, *357*, 266–281; (d) Holick, M. F. *Photobiology of Vitamin D. In Vitamin D*, 4th ed.; Elsevier: **2018**; pp 44−55.

12. Kweon, B.; Blank, L.; Soika, J.; Messara, A.; Daniliuc, C. G.; Gilmour, R. Regio- and Stereo-Selective Isomerization of Borylated 1,3-Dienes Enabled by Selective Energy Transfer Catalysis. *Angew. Chem. Int. Ed.* **2024**, *63*, e202404233.

13. Blank, L.; Kim, J.; Daniliuc, C. G.; Goetzinger, A.; Müller, M.-A.; Schütz, J.; Wuestenberg, B.; Gilmour, R. Deconjugative Photoisomerization of Cyclic Enones. *J. Am. Chem. Soc.* **2025**, *147*, 10023–10030.

14. For examples on boron-enabled geometric isomerization of alkenes, see: (a) Molloy, J. J.; Schäfer, M.; Wienhold, M.; Morack, T.; Daniliuc, C. G.; Gilmour, R. Boron-Enabled Geometric Isomerization of Alkenes via Selective Energy-Transfer Catalysis. *Science* **2020**, *369*, 302–306; (b) Wienhold, M.; Kweon, B.; McLaughlin, C.; Schmitz, M.; Zähringer, T. J. B.; Daniliuc, C. G.; Kerzig, C.; Gilmour, R. Geometric Isomerisation of Bifunctional Alkenyl Fluoride Linchpins: Stereodivergence in Amide and Polyene Bioisostere Synthesis. *Angew. Chem. Int. Ed.* **2023**, *62*, e202304150; (c) Zähringer, T. J. B.; Wienhold, M.; Gilmour, R.; Kerzig, C. Direct Observation of Triplet States in the Isomerization of Alkenylboronates by Energy Transfer Catalysis. *J. Am. Chem. Soc.* **2023**, *145*, 21576–21586.

15. (a) Coca, A. *Boron Reagents in Synthesis*, ACS Symposium Series 1236, American Chemical Society, Washington, **2016**; (b) Fyfe, J. W. B.; Watson, A. J. B. Recent Developments in Organoboron Chemistry: Old Dogs, New Tricks. *Chem* **2017**, 3, 31–55; (c) Fernández, E. *Advances in Organoboron Chemistry towards Organic Synthesis*, Thieme, Stuttgart, **2020**.

16. For examples on the photoisomerization of β-ionyl derivatives, see: (a) Mayo, P. D.; Stothers, J. B.; Yip, R. W. The Irradiation of β-Ionone. *Can. J. Chem.* **1961**, *39*, 2135–2137; (b) Mousseron, M. Isomérisation photochimique de systèmes polyéniques. *Pure Appl. Chem.* **1964**, *9*, 481–492; (c)

Ramamurthy, V.; Liu, R. S. H. Photochemistry of Polyenes. IX. Excitation, Relaxation, and Deactivation of Dienes, Trienes, and Higher Polyenes in the Vitamin A Series in the Sensitized Isomerization Reaction. *J. Am. Chem. Soc.* **1976**, *98*, 2935–2942; (d) Ramamurthy, V.; Liu, R. S. H. Sigmatropic Hydrogen Migration and Electrocyclization Processes in Compounds in the Vitamin A Series. Photochemistry of Polyenes. X. *J. Org. Chem.* **1976**, *41*, 1862–1867; (e) Liu, R. S. H.; Asato, A. E. Photochemistry and Synthesis of Stereoisomers of Vitamin A. *Tetrahedron* **1984**, *40*, 1931–1969; (f) Livingstone, K.; Tenberge, M.; Pape, F.; Daniliuc, C. G.; Jamieson, C.; Gilmour, R. Photocatalytic *E* → *Z* Isomerization of β-ionyl Derivatives. *Org. Lett.* **2019**, *21*, 9677–9680.

17. a) Johnson, F. Allylic Strain in Six-Membered Rings. *Chem. Rev*. **1968**, *68*, 375-413; (b) Hoffmann, R. W. Allylic 1,3-Strain as a Controlling Factor in Stereoselective Transformations. *Chem. Rev.* **1989**, *89*, 1841–1860; (c) Hoffmann, R. W. Flexible Molecules with Defined Shape – Conformational Design. *Angew. Chem. Int. Ed*. **1992**, *31*, 1124-1134.

18. Büchi, G.; Yang, N. C. Light-Catalyzed Organic Reactions. VI. The Isomerization of Some Dienones. *J. Am. Chem. Soc.* **1957**, *79*, 2318–2323.

19. Solans, M. M.; Basistyi, V. S.; Law, J. A.; Bartfield, N. M.; Frederich, J. H. Programmed Polyene Cyclization Enabled by Chromophore Disruption. *J. Am. Chem. Soc.* **2022**, *144*, 6193–6199.

20. Nagao, K.; Yamazaki, A.; Ohmiya, H.; Sawamura, M. Phosphine-Catalyzed Anti-Hydroboration of Internal Alkynes. *Org. Lett.* **2018**, *20*, 1861–1865.

21. X-ray data: CCDC 2467358 (for ***Z*-28**), CCDC 2467359 (for ***E*-28**) and CCDC 2467357 (for ***Z*-18**) contain the supplementary crystallographic data for this paper. These data are provided free of charge by the joint Cambridge Crystallographic Data Centre and Fachinformationszentrum Karlsruhe Access Structures service.

22. For examples of suprafacial thermal [1,5]-hydrogen shifts, see: (a) Roth, W. R.; König, J. Wasserstoffverschiebungen, IV. Kinetischer Isotopeneffekt der 1.5-Wasserstoffverschiebung im *cis*-Pentadien-(1.3). *Justus Liebigs Ann. Chem.* **1966**, *699*, 24–32; (b) Hess, B. A.; Baldwin, J. E. [1,5]-Sigmatropic Hydrogen Shifts in Cyclic 1,3-Dienes. *J. Org. Chem.* **2002**, *67*, 6025–6033.

23. Although rarely encountered, antarafacial [1,5]-hydrogen shifts can occur under photochemical conditions. For an example see: Kiefer, E. F.; Tanna, C. H. Alternative Electrocyclic Pathways. Photolysis and Thermolysis of Dimethylallene Dimers. *J. Am. Chem. Soc.* **1969**, *91*, 4478–4480.

24. (a) Kumar, N.; Reddy, R. R.; Eghbarieh, N.; Masarwa, A. α-Borylalkyl Radicals: Their Distinctive Reactivity in Modern Organic Synthesis. *Chem. Commun.* **2019**, *56*, 13–25; (b) Kischkewitz, M.; Friese, F. W.; Studer, A. Radical-Induced 1,2-Migrations of Boron Ate Complexes. *Adv. Synth. Catal.* **2020**, *362*, 2077–2087; (c) Marotta, A.; Fang, H.; Adams, C. E.; Sun Marcus, K.; Daniliuc, C. G.; Molloy, J. J. Direct Light-Enabled Access to α-Boryl Radicals: Application in the Stereodivergent Synthesis of Allyl Boronic Esters. *Angew. Chem. Int. Ed.* **2023**, *62*, e202307540.

25. Huang, Q.; Hu, M.-Y.; Zhu, S.-F. Cobalt-Catalyzed Cyclization/Hydroboration of 1,6-Diynes with Pinacolborane. *Org. Lett.* **2019**, *21*, 7883–7887.

26. (a) Smoum, R.; Rubinstein, A.; Dembitsky, V. M.; Srebnik, M. Boron Containing Compounds as Protease Inhibitors. *Chem. Rev.* **2012**, *112*, 4156–4220; (b) Das, B. C.; Adil Shareef, M.; Das, S.; Nandwana, N. K.; Das, Y.; Saito, M.; Weiss, L. M. Boron-Containing Heterocycles as Promising Pharmacological Agents. *Bioorg. Med. Chem.* **2022**, *63*, 116748; (c) Grams, R. J.; Santos, W. L.; Scorei, I. R.; Abad-García, A.; Rosenblum, C. A.; Bita, A.; Cerecetto, H.; Viñas, C.; Soriano-Ursúa, M. A. The Rise of Boron-Containing Compounds: Advancements in Synthesis, Medicinal Chemistry, and Emerging Pharmacology. *Chem. Rev.* **2024**, *124*, 2441–2511.